Reactions of $Cu^+(^1S,^3D)$ and $Au^+(^1S,^3D)$ with CH_3Br

William S. Taylor,* Jody C. May, and Aimee S. Lasater

Department of Chemistry, University of Central Arkansas, Conway, Arkansas 72035

Received: May 31, 2002; In Final Form: November 19, 2002

The reactions of $Cu^+(^1S,^3D)$ and $Au^+(^1S,^3D)$ with CH_3Br have been carried out in the gas phase at 150 K using a drift cell. State specific product channels were identified by observing the occurrence of product ions when ionization conditions were manipulated to either produce or eliminate excited states of the two metal ions. Reactant ion state distributions were determined by electronic state chromatography. State-specificity was confirmed by correlating reactant and product arrival time distributions. Association products correlate to singlet metal ion states for both Cu^+ and Au^+. Additionally, $Cu^+(^3D)$ participates in association under these conditions. The ^3D state of both metals exhibits Br abstraction, and CH_3 is abstracted by $Au^+(^3D)$. Formation of $AuCH_2^+$ exclusively via $Au^+(^1S)$ is also indicated. State-specificity with respect to bimolecular channels for both metals is consistent with thermochemical requirements and formal conservation of electron spin. Parallel formation of $AuCH_2^+$ and $Au^+ \cdot CH_3Br$ suggests a mechanism leading to HBr elimination that involves a long-lived insertion intermediate.

Introduction

An intriguing characteristic of metal ions is their ability to activate σ-bonds, resulting in species that either occur as, or serve as models for intermediates in catalytic mechanisms. In such mechanisms, typically unreactive (but often abundant) molecules such as methane are functionalized to yield useful products. Such catalytic intermediates are coordinatively unsaturated with respect to the metal, and are therefore extremely reactive. As a result, detailed information regarding the behavior of these open-shell species is often difficult to obtain in condensed phases. Furthermore, the presence of solvent molecules and other ligating species within the coordination sphere of the metal can dramatically influence its reactivity. Gas-phase studies of the reactions of transition metal ions with organic compounds can yield insights into intrinsic reactivity while avoiding these complicating effects.

A battery of techniques has been brought to bear in the examination of gas-phase metal ion chemistry, resulting in a wealth of thermochemical and dynamic information. These studies have thoroughly illustrated that the outcomes of these reactions can be dramatically influenced by the electronic state of the metal, often to the extent that certain states become unreactive regardless of favorable energetics for a given product channel.[1−7] An often-cited goal of gas-phase transition metal ion studies is that this electronic sensitivity might be exploited to selectively control formation of desired products. Research into this electronic dependence has revealed that state-specificity can be understood in terms of both orbital occupancy requirements for bonding; i.e., electron configuration, and conservation of electron spin. Orbital occupancy arguments deal with correlations between atomic orbital configurations and molecular orbitals in intermediates or products, which influence the ability of the metal to participate in bond activation. This process requires that an orbital of the appropriate symmetry on the metal accept electron density from the bond. For first-row ions, the large 4s orbital largely performs this function.[1,3,5] In addition, the configuration of the metal ion can also affect reactivity via the attractive/repulsive nature of the long-range interaction potential between the ion and the neutral.

The influence of electron spin on the accessibility of specific product channels has been demonstrated by numerous studies of C−H bond activation in hydrocarbons by first-row transition metal ions.[4,5] In this framework, reaction pathways are allowed in which electron spin is conserved from reactants to products. Conversely, reactions that do not conserve spin proceed either inefficiently or not at all, even if product formation is energetically favorable. Apparent exceptions to spin conservation can arise when coupling between reaction surfaces allows spin changes to occur.[8−10] Changes in spin frequently result in barriers that lower the efficiency of the reaction.

Though these ideas have been reasonably successful in explaining patterns of reactivity for first-row ions, it is not clear that the same rules apply to heavier ions due to several additional contributing effects. Relativistic effects in the third-row act to decrease the size of the 6s orbital and increase the size of the 5d orbitals. This is manifested in the ability of these heavy ions to form stronger covalent bonds through greater orbital overlap.[11] Further, the similar sizes of the 5d and 6s orbitals make sd hybridization less costly energetically. As a consequence of these characteristics, more exothermic product channels are available in systems involving third-row ions. Large spin−orbit effects in third-row ions mean that the usefulness of spin as a predictive tool becomes less certain. Indeed, the literature provides mixed results as to the influence of spin on reaction outcomes. For example, efficient dehydrogenation of CH_4 by Pt^+ has been shown to proceed via a mechanism in which spin is conserved;[12] however, the spin-forbidden photodissociation of $AuCH_2^+(^1A_1)$ to $Au^+(^1S)$ and $CH_2(^3B_1)$ has also been reported.[13] This ambiguity with respect to conservation of electron spin suggests that other factors may play a role in regulating the outcomes of reaction involving heavy ions, and clearly indicates the need for further examples of state-selected systems for heavy ions. Dehydrogenation reactions of the third-row ions Hf^+-Au^+ with CH_4 exhibit patterns of reactivity consistent with the idea that particular *configurations* are required for reaction;[14−16] however,

10.1021/jp026218k CCC: $25.00
Published on Web 03/11/2003

comparatively few studies have been reported in which the spin states of third-row ions have been definitively specified.

In this paper, we describe the state-specific reactions of Cu^+-(^1S), Cu^+(^3D), Au^+(^1S), and Au^+(^3D) with CH_3Br. These two metals are well-suited for this examination for several reasons. Both possess a limited number of low-lying excited states as compared with earlier transition metal ions. Thus, in the absence of the ability to selectively populate a given state this reduces the number of states sampled for subsequent reaction and simplifies the reaction analysis. Of particular benefit with respect to Au^+ is the fact that there is no overlap of the spin−orbit states of the ground and lowest excited (^3D) L−S terms, which could also complicate determinations of state-specificity. Likewise, there is no overlap of the ^3D spin−orbit states with those of the second excited L−S term ^1D. Further, the ^1S and ^3D states possess different electronic configurations ($3d^{10}$ and $3d^94s^1$ for Cu^+; $5d^{10}$ and $5d^96s^1$ for Au^+). This allows them to be distinguished on the basis of differences in their mobilities in He using electronic state chromatography.[17] Because the requirements for reaction of first-row ions are better understood, Cu^+ provides a useful basis for comparison. Numerous studies of the behavior of Cu^+(^1S) have been reported.[18−22] In addition, state-specific comparisons have highlighted differences in the chemistry of Cu^+(^1S) and Cu^+(^3D).[23,24] Au^+ is known to exhibit efficient elimination of HBr from CH_3Br;[25,26] thus, simple reaction systems are available in which the influence of electronic state on σ-bond activation can be examined for this metal.

Experimental Section

Experiments were carried out using a drift cell apparatus described in detail previously.[27] Briefly, this instrument incorporates a sputtering dc glow discharge ion source to produce metal ions that are then directed to a 4.0 cm drift cell containing 3−5 Torr of He. Typical metal ion signals measured under these conditions are in the range of 10^3-10^4 cps. Temperature control of the drift cell is accomplished via a copper jacket through which heated or cooled gases can be circulated. In this work, low temperatures necessary for the determination of reactant ion states were achieved by introducing liquid nitrogen into the copper jacket. Temperatures within the drift cell are monitored using a Pt−RTD (resistance temperature device). Ions are drawn through the drift cell via a weak electric field. For the result reported here, the field strength was adjusted such that E/N was approximately 5 Td (1 Td = 1×10^{-17} cm^2·V). Ions exiting the drift cell are mass-analyzed via a quadrupole mass filter, and subsequently detected using an electron multiplier. The output of the electron multiplier is then sent to a multichannel scaler, and the data can then be displayed in a number of formats on a laboratory computer.

In this work, specific configurations of Cu^+ and Au^+ ions produced in the glow discharge were identified within the drift cell using a technique called electronic state chromatography (ESC), which characterizes them on the basis of the their mobilities in He.[17] ESC is most effective in distinguishing between electronic configurations differing significantly in size, such as those that differ by either the presence or absence of an s electron. The larger size of the s orbital results in a greater repulsive interaction between the ion and the He bath gas, which reduces the number of capture-collisions. In terms of the first-row ions, this means that ions with $3d^{n-1}4s^1$ configurations have higher mobilities in the bath gas than those with $3d^n$ configurations. As a consequence, a pulse containing a given metal ion in both configurations will be separated within the drift cell such that the higher mobility configuration arrives at the detector first. Thus, configurations of sufficiently different mobilities appear as different peaks in an arrival time distribution (ATD). Ion mobilities used in assigning configurations were obtained from the ATD's by measuring the flight time of the different configurations as a function of the reciprocal of the drift voltage.

ESC analysis of Cu^+ and Au^+ extracted from the discharge indicate the presence of two configurations for both ions. Mobility measurements indicate that these correspond to $3d^{10}$ and $3d^94s^1$ for Cu^+ and $5d^{10}$ and $5d^96s^1$ for Au^+. A previous analysis of excited states formed in the glow discharge suggests that this ion source is capable of producing excited metal ion states with energies up to approximately 11.8 eV above the atom ground state.[28] For Cu^+, this energy range includes the $^1S(3d^{10})$, $^3D(3d^94s^1)$, and $^1D(3d^94s^1)$ states. The low-mobility feature in our Cu^+ ATD's is undoubtedly the ^1S ground state, but because the first and second excited states are indistinguishable on the basis of their mobilities, we cannot rule out the presence of both within the high-mobility feature. Our previous examination of ionization/excitation within the discharge has suggested that excited atomic ions extracted from the discharge are produced primarily by an electron impact process and, in the absence of any preferential depletion mechanism(s), the relative populations of the excited metal ions will be dependent on the electron energy distribution function at the point of sampling within the discharge.[28] Thus, although some amount of Cu^+(^1D) may be present in the $3d^94s^1$ (high mobility) feature, it is likely that the major contributor to this configuration is the energetically more accessible ^3D state. A similar analysis of Au^+ ATD's indicates the presence of $5d^{10}$ and $5d^96s^1$ configurations. On the basis of energetic constraints, we assign the low-mobility feature as the $^1S_0$ ground state whereas the high-mobility feature contains some mixture of both the $^3D_3$ and $^3D_2$ states. Relative amounts of the two configurations for both metals were controlled by variations in discharge parameters as has been described previously.[28] Unless otherwise specified, all ATD's were collected using a pulse width of 5 μs and at drift cell temperatures of approximately 150 K to enhance ESC resolution.

Gold cathodes used as sputter targets in the discharge were purchased from Alfa Æsar in the form of 3.0 mm rods with a purity of 99.9985%. Copper cathodes were fashioned from used gaskets into 5.0 mm diameter rods. Neon and argon used as discharge gases were obtained with purities of 99.9995% and 99.999%, respectively. Helium used as the buffer gas in the drift cell had a purity of 99.9999%. Methyl bromide used in these reactions was 99% pure. He and Ar were obtained from Air Products Inc. whereas Neon and CH_3Br were purchased from Matheson Tri-Gas Inc.

Results and Discussion

Products formed in the reactions examined in this study include all of those generalized by reactions 1−4 shown in Scheme 1. Initial interaction of the metal ion with CH_3Br results in the formation of an energized adduct species that, depending on the specific reacting system, can sample one or more of the four product channels, or dissociate back into reactants.

Formation of association products via process 1 represents a large portion of the total product formation for both metal ions under the multicollisional conditions present within the drift cell. Branching into this product channel is dependent upon the He pressure in the drift cell as well as on the efficiency (β) of each stabilizing collision. As we will show, association products arise almost exclusively from the ground states of both metal ions with this neutral, whereas bimolecular product formation occurs

SCHEME 1

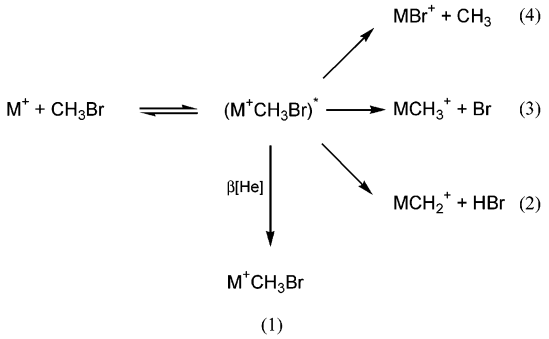

via both ground and excited states. Access to bimolecular product channels was dependent upon the populations of reactant ion excited states, which were influenced by ionizing and sampling parameters within the discharge. In this work, experimental conditions were such that bimolecular product formation contributes less than 20% to the total product ion signal for both metal ion systems. Nevertheless, the bimolecular products are of interest here because they are clearly the result of molecular rearrangements induced by the metal ion, whereas association products could simply represent electrostatically bound complexes.

As expected, Au^+ was observed to be the more reactive of the two metals, exhibiting evidence of reactions 2−4 in addition to association. In a recent study of the Au^+/CH_3Br system, Brown et al. report no evidence of elimination of Br or CH_3 when the Au^+ ions were thermalized prior to reaction.[26] Our results indicate that these reactions occur exclusively from excited Au^+ states. Chowdhury and Wilkins also noted CH_2Br^+ as a minor (1%) product in addition to reactions 1 and 2.[25] We observe this species as well, but because other species capable of reacting with CH_3Br to yield CH_2Br^+ are produced by the discharge, we cannot conclusively assign Au^+ as its precursor. Reaction 4 was the only bimolecular process displayed by Cu^+. Secondary association products were observed for all major product channels.

State-Specificity. The reactivity of each metal ion state was initially assessed by collecting reactant ATD's in the presence of varying concentrations of CH_3Br in He. For this work neutral mole fractions were on the order of 10^{-4} at a total He pressure of 3.0 Torr. For both metals, ATD's obtained in the presence of varying amounts of CH_3Br clearly indicate that both ^1S and ^3D states are depleted. Figure 1 illustrates this for Cu^+, where there is a preference for the ^1S state under the conditions used in this study. Similar determinations with Au^+ indicate that both excited and ground states are consumed with similar efficiencies. State-specificity with respect to product formation was determined using two methods: (1) acquisition of product mass spectra while manipulating reactant ion state distributions and (2) correlating reactant and product ATD's. In the first method, the discharge conditions were first adjusted such that production of $M^+(^3D)$ was minimized or eliminated. A continuous beam of the reactant ion was then injected into the drift cell containing CH_3Br/He mixture described above. Mass spectra accumulated under these conditions were then compared to those obtained when the discharge was adjusted to produce the ^3D state in addition to the ground state.

Product ATD's were correlated to reactant ion ATD's using a method outlined previously.[29] The reactant ion ATD is first collected under the same drift cell conditions as the reaction of interest. A small amount of the reactant neutral is then admitted into the drift cell and the mass filter is tuned to the desired

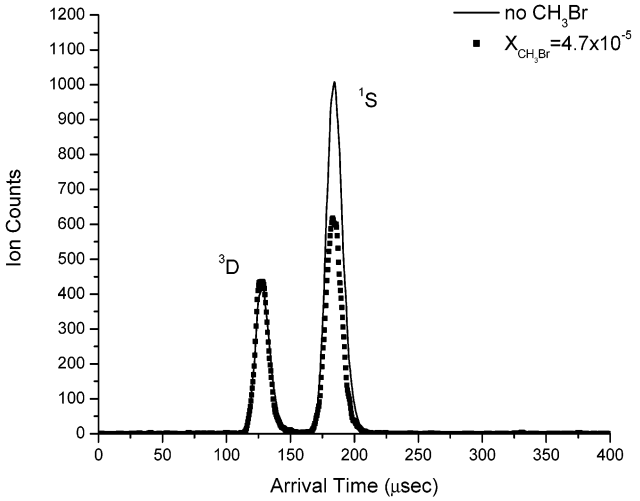

Figure 1. Cu^+ ATD's with and without CH_3Br present in the drift cell. $T = 147$ K; $E/N = 5.1$ Td. ATD's were obtained using collection times that resulted in equal intensities for the ^3D state.

TABLE 1: Bimolecular Product Summary

metal ion	state energy[a]	product channel	thermochemistry[b]	ΔΣ	obsd?
$(^1S)Cu^+$	0.00	$CuCH_2^+ + HBr$	+129	0	N
		$CuBr^+ + CH_3$[c]		0, ±1	N
		$CuCH_3^+ + Br$	+182	0, ±1	N
$(^3D)Cu^+$	2.81	$CuCH_2^+ + HBr$	−142	±1	N
		$CuBr^+ + CH_3$[c]		0, ±1, ±2	Y
		$CuCH_3^+ + Br$	−89	0, ±1, ±2	N
$(^1S_0)Au^+$	0.00	$AuCH_2^+ + HBr$	+13	0	Y
		$AuBr^+ + CH_3$	+125	0, ±1	N
		$AuCH_3^+ + Br$	+102	0, ±1	N
$(^3D_{3,2})Au^+$	1.86, 2.19	$AuCH_2^+ + HBr$	−167, −198	±1	N
		$AuBr^+ + CH_3$	−54, −86	0, ±1, ±2	Y
		$AuCH_3^+ + Br$	−77, −109	0, ±1, ±2	Y

[a] In eV. [b] In kJ/mol; values separated by commas indicate reaction thermochemistry relative to more than one spin−orbit state. [c] $Cu-Br^+$ binding energy not known.

product ion mass while the reactant ion beam is pulsed. The ATD's for both species are then corrected to account for differences in flight times through the quadrupole, and then overlaid. The reactant ion can be converted into the product at any point within the drift cell, but a product ion formed near the exit of the drift cell will exhibit a flight time characteristic of the reactant ion producing it. Thus, the ATD of a product ion with a lower mobility than the reactant (as was the case for all product ions discussed here due to the incorporation of the ligand) will originate at the same time as the reactant ion producing it. In this way, the metal ion state responsible for the formation of each was identified. State-specific reactivity for both metal ions is summarized in Table 1 for the bimolecular products observed here, along with the available thermochemistry[13,30,31] and overall change in spin for each product channel.

Copper. Although association proceeds mainly from $Cu^+(^1S)$, the ATD for $Cu^+ \cdot CH_3Br$ shown in Figure 2a indicates that some portion of this product correlates to $Cu^+(^3D)$ at 150 K. This is confirmed by the disappearance of the product feature at 150 μs correlating to $Cu^+(^3D)$ when the discharge is adjusted to eliminate the excited Cu^+ state (shown in Figure 2b). Association arising from $Cu^+(^3D)$ could be an indication of coupling between the singlet and triplet reaction surfaces via intersystem crossing (ISC). If occurring, this would facilitate quenching of $Cu^+(^3D)$ by CH_3Br to $Cu^+(^1S)$, which subsequently yields the stabilized adduct. We have observed this behavior previously in the interaction of $Cu^+(^3D)$ with C_2H_4;[32] however, our results argue against this possibility in this case. Provided

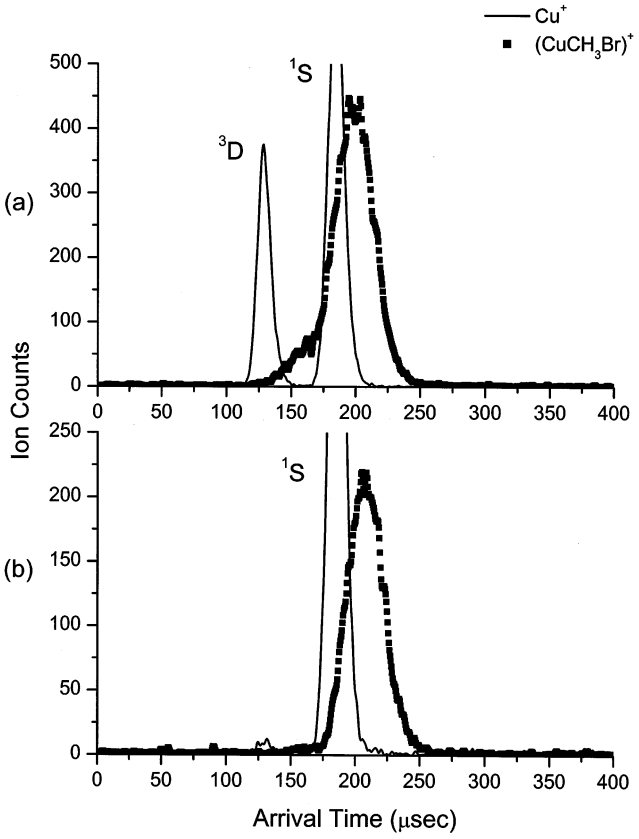

Figure 2. Cu^+ and $Cu^+ \cdot CH_3Br$ ATD's with ionization conditions adjusted to either (a) enhance or (b) suppress production of $Cu^+(^3D)$. $T = 146$ K; $E/N = 5.0$ Td; $X_{CH_3Br} = 5.7 \times 10^{-5}$.

that quenching occurs early on the triplet reaction surface, such a mechanism would be evidenced by bridging within the Cu^+ ATD. This feature arises when high-mobility ions are converted to low-mobility ions within the drift cell due to competitive dissociation of the ground state association complex. In these cases, the deactivated species exhibits an arrival time intermediate between that of the low-mobility species and the high-mobility species. Examples of such behavior have also been reported previously for Fe^+ and Mn^+.[17] The Cu^+ ATD's in the presence of CH_3Br in Figure 1 show no evidence of intermediate flight times, and we therefore reject the quenching mechanism. It is more plausible that association is proceeding directly from both Cu^+ states under these conditions, with the more repulsive character of the interaction involving the $3d^94s^1$ configuration yielding a weakly bound complex. This hypothesis is given additional weight by noting that contribution to the excited state association product disappears when the reaction is run at room temperature.

Bimolecular product formation summarized in Table 1 in the Cu^+/CH_3Br system is consistent with the requirement of conservation of spin together with the known thermochemical requirements for each product channel. Electronic excitation of the metal ions by the discharge notwithstanding, reaction conditions in the drift cell are best described as "near-thermal", with some degree of translational excitation imparted by the drift field.[27] This effect is usually small enough such that only exothermic processes are observed to occur. The lack of formation of $CuCH_2^+$ (singlet) and $CuCH_3^+$ (doublet) can be partially understood in this light. Although formation of both species is spin-allowed from the ground state, the thermochemistry of these product channels is unfavorable under the conditions of these experiments.[30] Notably, both product channels are exothermic via $Cu^+(^3D)$; however, formation of $CuCH_2^+$ is spin-forbidden from $Cu^+(^3D)$. Formation of $CuCH_3^+$ via $Cu^+(^3D)$ is spin-allowed in addition to being thermochemically possible. We therefore interpret its absence in the presence of this Cu^+ state as an indication this product channel is not efficient enough to be competitive with $CuBr^+$ formation.

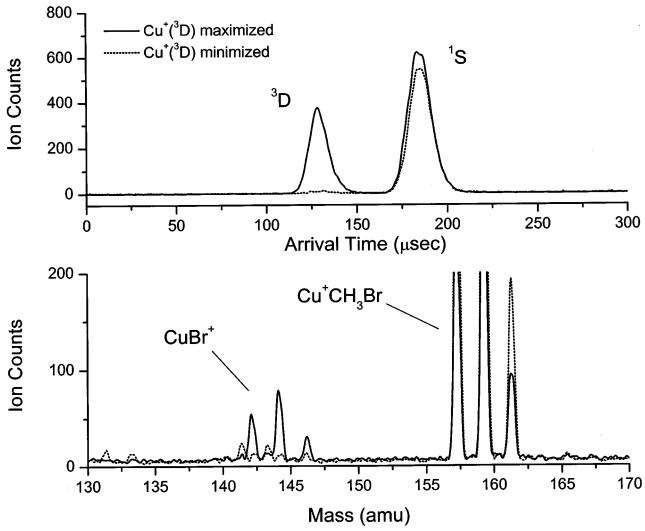

Figure 3. Cu^+ ATD's and corresponding mass spectra for reaction with CH_3Br. Ionization conditions were manipulated to either enhance or suppress production of $Cu^+(^3D)$. $T = 146$ K; $E/N = 5.0$ Td; $X_{CH_3Br} = 5.7 \times 10^{-5}$.

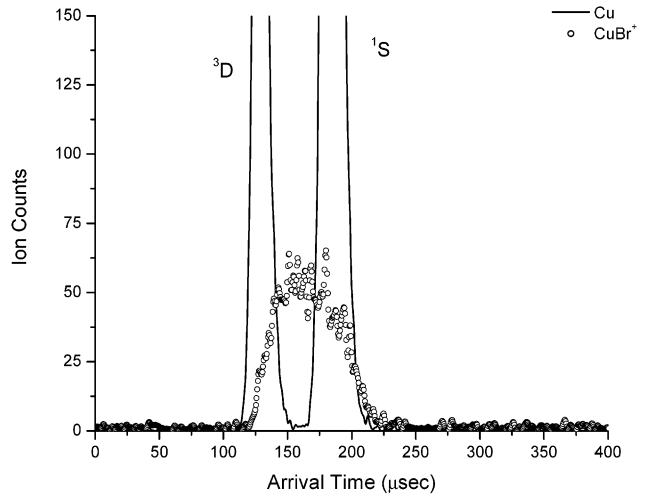

Figure 4. Cu^+ and $CuBr^+$ ATD's illustrating the correlation between $CuBr^+$ and $Cu^+(^3D)$. $T = 146$ K; $E/N = 5.0$ Td; $X_{CH_3Br} = 4.7 \times 10^{-5}$. The maximum in the product ATD is displaced relative to that of $Cu^+(^3D)$ due to it's lower mobility.

The ground electronic state of $CuBr^+$ is most likely doublet, because this correlates to $Cu^+(^1S)$ and $Br(^2P)$ ground state species. Formation of ground state $CuBr^+$ is therefore formally spin-allowed from either Cu^+ state; however the thermochemistry is unfavorable via $Cu^+(^1S)$. Figure 3 shows spectra for the Cu^+/CH_3Br system in which discharge conditions have been manipulated to either allow or suppress production of excited Cu^+. Though the association product is formed regardless of the presence or absence of excited Cu^+, these spectra clearly indicate that formation of $CuBr^+$ only occurs in the presence of $Cu^+(^3D)$. This is confirmed by the product ATD for $CuBr^+$ shown in Figure 4, which correlates to the high-mobility Cu^+ feature.

Formal conservation of spin does not necessarily preclude spin changes within mechanisms. The recently described

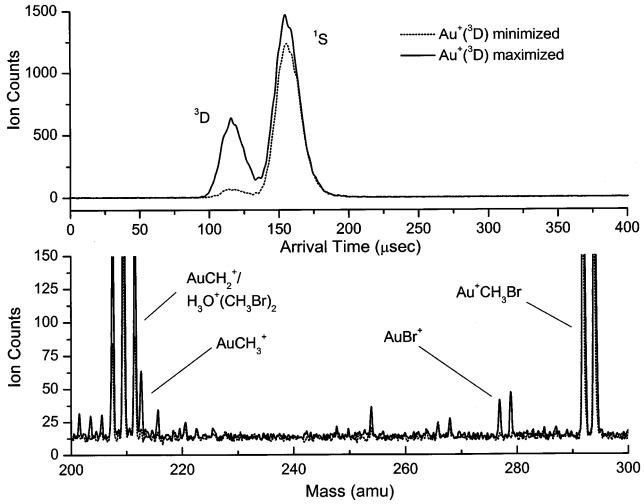

Figure 5. Au^+ ATD's and associated mass spectra for reaction with CH_3Br. $T = 150$ K; $E/N = 4.9$ Td; $X_{CH_3Br} = 4.6 \times 10^{-5}$.

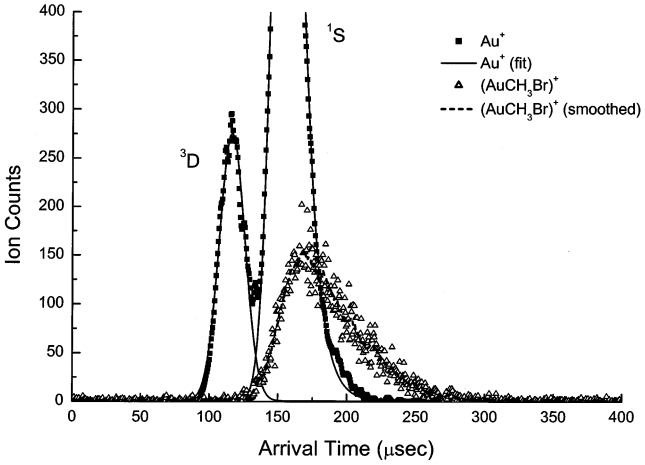

Figure 6. Au^+ and $Au^+ \cdot CH_3Br$ ATD's. Au^+ ATD's fit to Gaussians; smoothed $Au^+ \cdot CH_3Br$ data (dashed line) shown for clarity. $T = 151$ K; $E/N = 4.9$ Td; $X_{CH_3Br} = 4.7 \times 10^{-5}$.

phenomenon of two-state reactivity (TSR) includes examples in which spin is conserved overall, yet the low-energy pathway to reaction involves two spin changes.[10] Although the ordering of the Cu^+ spin states does not meet the requirements of TSR, as has been described, it is difficult on the basis of these results alone to speculate regarding mechanistic details. Certainly, one can envision scenarios where curve-crossings could occur. For example, the reaction of Cu^+ with H_2O to form CuO^+ represents a case in which the triplet and singlet surfaces cross as a result of a reversal in the relative order of the high- and low-spin states in the products from that of the reactants.[24] We note, however, that this does not occur with respect to the formation of $CuCH_2^+$; therefore the lack of formation of the carbene from $Cu^+(^3D)$ despite favorable thermochemistry suggests that the singlet and triplet surfaces are not coupled. This is also in accordance with the behavior described above regarding the formation of association products from both Cu^+ states. Thus, the weight of the evidence supports the idea that the two Cu^+ reaction surfaces do not interact. This would be consistent with other examples of reactions of Cu^+ that indicate conservation of spin for both $Cu^+(^1S)$ and $Cu^+(^3D)$,[23] as well as the behavior of first-row ions in general.

Taken in this light, formation of the radical products described by reaction 4 is consistent with a process occurring diabatically on a high-spin surface.[10] This implies that formation of $CuBr^+$ proceeds through Br abstraction rather than via formation of an insertion complex requiring inversion of spin.

Gold. Product mass spectra collected with and without $Au^+(^3D)$ are given in Figure 5, which illustrate all four of the product channels exhibited by this metal. Like the Cu^+/CH_3Br system, the association product in this reaction appears in the mass spectrum regardless of whether $Au^+(^3D)$ is present during the reaction. Thus, analysis of product ATD's is necessary to evaluate the contribution of the excited state to formation of stabilized adducts. This is shown in Figure 6. Whereas $Cu^+(^3D)$ participates in association at low temperatures, association with Au^+ proceeds exclusively from the ground state. This is a notable difference in the behavior of the two metals because the long-range interaction potentials between the two Au^+ states and CH_3Br should not differ as much as those for the two Cu^+ states with this neutral. This occurs because the difference in size of the two Au^+ configurations is not as great as that for the analogous Cu^+ configurations.[15,33] Evidence of this characteristic can be seen in the differences in the interactions of each Au^+ state with He, as exhibited by the lower resolution of the Au^+ ATD as compared with that of Cu^+. Thus, if association via ground state Au^+ occurs, we would expect the excited state to behave similarly, provided no competing processes are available with significantly higher efficiencies. Failure of $Au^+(^3D)$ to form stabilized adducts must then be an indication that the bimolecular product channels proceeding from this Au^+ state do not contain sufficiently energetic barriers to allow association to compete.

The spectra in Figure 5 also show that, as in the case of Cu^+, $AuBr^+$ is formed exclusively in the presence of the $Au^+(^3D)$ state. This result is consistent with the recent observation that Br abstraction by thermalized Au^+ does not occur.[26] We further observe that $AuCH_3^+$ appears in the presence of $Au^+(^3D)$ as well. The $AuBr^+/AuCH_3^+$ branching ratio observed here is 1.4:1, indicating that the two processes occur with similar efficiencies. We note that neither of these products was observed by Chowdhury and Wilkins, suggesting that insufficient $Au^+(^3D)$ was present in this earlier study to form these species.[25] Product ATD's obtained at 150 K indicate that $AuBr^+$ and $AuCH_3^+$ both originate from the same precursor and both correlate to the higher mobility (^3D) feature of the Au^+ ATD.

Because formation of both products is spin-allowed via both $Au^+(^1S)$ and $Au^+(^3D)$, this cannot be used as a criterion for state-specificity in this case. Rather, state-specificity for these products is simply the result of favorable thermochemistry relative to $Au^+(^3D)$. Formation of $AuCH_2^+$ is likewise exothermic from $Au^+(^3D)$ and endothermic by 13 kJ/mol from the ground state.[13] As shown in Figure 5, elimination of HBr proceeds readily to yield $AuCH_2^+$ as the predominant bimolecular product regardless of whether $Au^+(^3D)$ is extracted from the discharge, thus implicating $Au^+(^1S)$ as a source of $AuCH_2^+$ in agreement with previously reported observations.[25] This indicates that some degree of translational heating is induced by the drift field. The participation (or lack thereof) of $Au^+(^3D)$ in the formation of gold carbene has not been previously established.[25,26] Because we have no means of selectively forming $Au^+(^3D)$ in the absence of $Au^+(^1S)$, a mass spectral analysis alone is insufficient to determine state-specificity for this product channel. Correlating ATD's for this product to those for Au^+ to establish state-specificity is problematic. At low temperatures, a species is formed in the drift cell with mass spectral peaks at 207, 209, and 211 amu in ratios consistent with the presence of two bromine atoms. H_3O^+ is produced in abundance by the discharge, and we therefore conclude that the species giving rise to these peaks is the cluster $H_3O^+ \cdot (CH_3-$

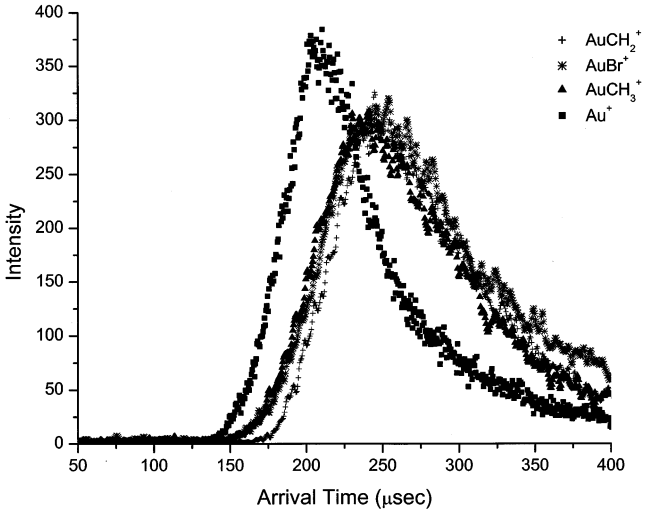

Figure 7. ATD's for Au^+, $AuCH_2^+$, $AuBr^+$, and $AuCH_3^+$. Au^+ pulse width = 5 μs; product pulse widths = 50 μs to improve sensitivity. T = 300 K; E/N = 4.9 Td; $X_{CH_3Br} = 6.2 \times 10^{-5}$ Au^+ ATD scaled by 0.33×. Tailing occurring at longer arrival times in these ATD's is attributable to the association and redissociation of the ions with other species in the drift cell.

$Br)_2$. Because 211 amu is also the mass of $AuCH_2^+$, ATD's of this mass under conditions where the cluster contributes are not useful. $H_3O^+ \cdot (CH_3Br)_2$ is not present at room temperature, but Au^+ ATD's under these conditions are not well-resolved. However, room-temperature ATD's for $AuBr^+$ and $AuCH_3^+$ (Figure 7) correlate very closely to each other, and to the beginning of the room-temperature Au^+ ATD, whereas the ATD for $AuCH_2^+$ originates 20 μs later. In light of the excellent agreement between the start times in the $AuBr^+$ and $AuCH_3^+$ ATD's, the delay in the start time of the $AuCH_2^+$ ATD strongly suggests that this species is not formed from the same Au^+ state as $AuBr^+$ and $AuCH_3^+$. Thus, it seems likely that formation of $AuCH_2^+(^1A_1)$ proceeds exclusively from $Au^+(^1S)$ despite favorable thermochemistry via $Au^+(^3D)$. This result appears to be analogous to that of $Cu^+(^3D)$ with respect to the formation of the carbene and is likewise consistent with a scenario in which the two reaction surfaces do not interact. Further, differences in the efficiencies of the product channels arising from the two Au^+ states point to independent mechanisms for bimolecular products arising from the two Au^+ states. Because association of $Au^+(^1S)$ occurs in addition to formation of $AuCH_2^+$ on the ground state surface, the lifetime of the intermediate leading to HBr elimination must be on the order of the time required to stabilize the adduct. On the basis of an ion-induced dipole interaction, the collision frequency for the interaction between He and $(Au^+ \cdot CH_3Br)^*$ under the conditions employed here is 10^8 s^{-1}. If we further assume a collision efficiency for He of 0.25 (four collisions required to remove the initial energy of interaction),[34,35] then the time required for collisional stabilization (and thus the lifetime of the intermediate leading to the formation of $AuCH_2^+$) is on the order of 40 ns. Given the requirements of conservation of spin and lifetime, a mechanism in which insertion of Au^+ into the CH_3-Br bond occurs seems reasonable. The lower efficiency of this process would be consistent with the interaction of the two closed-shell reactants in which a barrier to reaction arises from unpairing the electrons necessary to form two bonds in the insertion intermediate. With regard to the triplet surface, the fact that association involving $Au^+(^3D)$ does not occur indicates that the process(es) leading to formation of $AuBr^+$ and $AuCH_3^+$ occur much more rapidly, suggesting an independent mechanism. Given the behavior of $Cu^+(^3D)$, abstraction seems a likely possibility for $Au^+(^3D)$ as well.

Summary

The gas-phase reactions of the ^1S and ^3D states of Cu^+ and Au^+ with CH_3Br result in the formation of a variety of products. Observed processes for each metal ion exhibit evidence of bond activation, abstraction, and association under the conditions employed here. State-specific analysis of products reveals that $Cu^+(^1S)$ forms association products exclusively whereas $Cu^+(^3D)$ forms $CuBr^+$ in addition to association products. With one exception, access (or lack thereof) to bimolecular product channels in this system can be understood in terms of the known thermochemistry of each reaction along with conservation of electron spin. $CuCH_3^+$ is not observed via $Cu^+(^3D)$ even though thermochemical and spin requirements are favorable, suggesting unfavorable kinetic characteristics for this product channel. Spin-forbidden formation of $CuCH_2^+$ via $Cu^+(^3D)$ is not observed even though this reaction is exothermic by 142 kJ/mol. The overall behavior of this system is consistent with a mechanism in which $CuBr^+$ is formed on the triplet surface via abstraction. The behavior of the Au^+/CH_3Br system is more complex, exhibiting three bimolecular processes as well as association. State-specific product assignment reveals that $Au^+(^1S)$ participates in HBr elimination to yield $AuCH_2^+$ whereas $Au^+(^3D)$ yields $AuBr^+$ and $AuCH_3^+$. State-specificity with respect to these products is again consistent with thermochemical limitations and overall conservation of spin. Association proceeds exclusively from the ground state for this metal. Given the expectation of similar long-range interaction potentials for both ^1S and ^3D Au^+ with CH_3Br, the lack of association of this neutral with $Au^+(^3D)$ suggests that formation of $AuBr^+$ and $AuCH_3^+$ occurs on a time scale shorter than the time required to collisionally stabilize the triplet adduct. Conversely, observation of HBr elimination via $Au^+(^1S)$ in parallel with association points to a long-lived intermediate leading to formation of $AuCH_2^+$. Taken together, these observations are consistent with formation of $AuCH_2^+$ on the singlet surface via an insertion intermediate, whereas $AuBr^+$ and $AuCH_3^+$ are formed on the triplet surface via a more rapid abstraction process. Given the large spin−orbit coupling in Au^+ it would not be surprising to observe formation of products consistent with interactions between reaction surfaces. Yet, although a detailed examination of the mechanisms in these systems is clearly needed to evaluate the specific features of each reaction surface, the results reported here reveal no evidence of coupling between the two surfaces for either metal.

Acknowledgment. This work was supported in part by a Cottrell College Science Award of Research Corporation. Additional support for this research was provided by the National Science Foundation under Grant No. CHE-0078771.

References and Notes

(1) Armentrout, P. B.; Beauchamp, J. L. *Acc. Chem. Res.* **1989**, *22*, 315−321.

(2) Armentrout, P. B. In *Gas-Phase Inorganic Chemistry*; Russell, D. H., Ed.; Plenum: New York, 1989.

(3) Weisshaar, J. C. *Acc. Chem. Res.* **1993**, *26*, 213-219.

(4) Armentrout, P. B. *Annu. Rev. Phys. Chem.* **1990**, *41*, 313−344.

(5) Weisshaar, J. C. In *Advances in Chemical Physics*; Ng, C. Y., Baer, M., Ed.; Wiley and Sons Inc.: New York, 1992; Vol. LXXXII.

(6) Eller, K. E.; Schwarz, H. *Chem. Rev.* **1991**, *91*, 1121−1177.

(7) Armentrout, P. B. *Acc. Chem. Res.* **1995**, *28*, 430−436.

(8) Gidden, Jennifer; van Koppen, P. A. M.; Bowers, M. T. *J. Am. Chem. Soc.* **1997**, *119*, 3935−3941.
(9) van Koppen, P. A. M.; Bowers, M. T.; Haynes, C. L.; Armentrout, P. B. *J. Am. Chem. Soc.* **1998**, *120*, 5704−5712.
(10) Schröder, D.; Shaik, S.; Schwarz, H. *Acc. Chem. Res.* **2000**, *33*, 139−145.
(11) Ohanessian, G.; Brusich, M. J.; Goddard, W. A. *J. Am. Chem. Soc.* **1990**, *112*, 7179−7189.
(12) Zhang, Xiao-Guang; Liyange, R.; Armentrout, P. B. *J. Am. Chem. Soc.* **2001**, *123*, 5563−5575.
(13) Aguirre, F.; Husband, J.; Thompson, C. J.; Metz, R. B. *Chem. Phys. Lett.* **2000**, *318*, 466−470.
(14) Irikura, K. K.; Beauchamp, J. L. *J. Am. Chem. Soc.* **1991**, *113*, 2769−2770.
(15) Irikura, K. K.; Beauchamp, J. L. *J. Phys. Chem.* **1991**, *95*, 8344−8351.
(16) Irikura, K. K.; Goddard, W. A. *J. Am. Chem. Soc.* **1994**, *116*, 8733−8740.
(17) Kemper, P. R.; Bowers, M. T. *J. Phys. Chem.* **1991**, *95*, 5134−5146.
(18) Hoyau, S.; Ohanessian, G. *Chem. Phys. Lett.* **1997**, *280*, 266−272.
(19) Fisher, E. R.; Armentrout, P. B. *J. Phys. Chem.*, **1990**, *94*, 1674−1683.
(20) Georgiadis, R.; Fisher, E. R.; Armentrout, P. B. *J. Am. Chem. Soc.* **1989**, *111*, 4251−4262.
(21) Elkind, J. L.; Armentrout, P. B. *J. Phys. Chem.* **1986**, *90*, 6576−6586.
(22) Rue, C.; Armentrout, P. B.; Kretzschmar, I.; Schröder, D.; Schwarz, H. *J. Phys. Chem. A* **2002**, *106*, 9788−9797.
(23) Rodgers, M. T.; Walker, B.; Armentrout, P. B. *Int. J. Mass Spectrom. Ion Processes* **1999**, *182/183*, 99−120.
(24) Irigoras, A.; Elizalde, O.; Silanes, I.; Fowler, J. E.; Ugalde, J. M. *J. Am. Chem. Soc.* **2000**, *122*, 114−122.
(25) Chowdhury, A. K.; Wilkins, C. L. *J. Am. Chem. Soc.* **1987**, *109*, 5336−5343.
(26) Brown, J. R.; Schwerdtfeger, P.; Schröder, D.; Schwarz, H. *J. Am. Soc. Mass Spectrom.* **2002**, *13*, 485−492.
(27) Taylor, W. S.; Campbell, A. S.; Barnas, D. F.; Babcock, L. M.; Linder, C. B. *J. Phys. Chem. A* **1997**, *101*, 2654−2661.
(28) Taylor, W. S.; Spicer, E. M.; Barnas, D. F. *J. Phys. Chem. A* **1999**, *103*, 643−650.
(29) van Koppen, P. A. M.; Kemper, P. R.; Bowers, M. T. In *Organometallic Ion Chemistry*; Freiser, B. S., Eds.; Kluwer Academic Publishers: Boston, 1996.
(30) Armentrout, P. B.; Kickel, B. L. In *Organometallic Ion Chemistry*; Freiser, B. S., Eds.; Kluwer Academic Publishers: Boston, 1996.
(31) Holthausen, M. C.; Heinemann, C.; Cornehl, H. H.; Koch, W.; Schwarz, H. *J. Chem. Phys.* **1995**, *102*, 4931−4941.
(32) Taylor, W. S.; May, J. C. Unpublished results.
(33) Barnes, L. A.; Rosi, M.; Bauschlicher, C. W. *J. Chem. Phys.* **1990**, *93*, 609−624.
(34) Miasek, P. G.; Harrison, A. G. *J. Am. Chem. Soc.* **1975**, *97*, 714−720.
(35) Cates, R. D.; Bowers, M. T. *J. Am. Chem. Soc.* **1980**, *102*, 3994−3996.